Article

Solutions for better fitting Sigmoid-shaped functions to binary data

V.M.N.C.S. Vieira
MARETEC, Instituto Superior Técnico, Universidade Técnica de Lisboa, Lisboa, Portugal
E-mail: vasco.vieira@tecnico.ulisboa.pt

Received 23 April 2020; *Accepted 31 May 2020*; *Published 1 December 2020*

Abstract
Sigmoid-shaped curves are often used to estimate the probability of individuals surviving or becoming fecund (response: y) given some characteristic like age or size (predictor: x). However, the individual observations of y used to calibrate the curve are binary (0 or 1) because each individual either survived or not, and was fecund or not. A Matlab-based software is here demonstrated by fitting Gompertz and Weibull curves to the probabilities of the red alga *Gracilaria chilensis* becoming fecund depending on frond size. Different approaches are possible for parameter estimation, namely, minimizing the error sum of squares or maximizing the log-likelihood. Because neither have analytical solution, both were estimated by numerical methods as the Gauss-Newton, the Newton-Raphson, the Levenberg-Marquardt and the Matlab built-in fmincon function. Assuming x is bell-shape distributed, all these alternatives optimize the curve-fit to the bulk of the data i.e., in the middle of the curve. However, in this case the accuracy of the fit in the curve extremes was of utmost importance. A misfit could lead to a 124% change in estimated overall spore production. To balance the weight of curve sections, the observations were grouped into x classes and the curve was fit to their mean y. However, the small sizes of groups in the extremes rouse problems of numerical instability and uncertainty. The Gompertz curves were easier fit and could be done by any method while the Weibull curve could only be well fit by the Newton-Raphson method. Possible measures to improve convergence were the choice of initial guesses, decrease the step-size of the search, use a positive definite matrix re-directing the search or not using classes with too little observations inside.

Keywords Gompertz; Weibull; Newton-Raphson; Gauss-Newton; Levenberg-Marquardt; curvefit; sigmoid; binary.

Computational Ecology and Software
ISSN 2220-721X
URL: http://www.iaees.org/publications/journals/ces/online-version.asp
RSS: http://www.iaees.org/publications/journals/ces/rss.xml
E-mail: ces@iaees.org
Editor-in-Chief: WenJun Zhang
Publisher: International Academy of Ecology and Environmental Sciences

1 Introduction

Binary data (0 or 1) represents a problem common to many ecological and demographic studies, often demanding an intricate numerical analysis. Dependent variables like germination, survival and being fecund are observed for each individual as 0 (false) or 1 (true) and related with environmental continuous variables

like temperature (Dumur et al., 1990; Shafii and Price, 2001). In the present case, the data comprised the morphological and physiological state of fronds of the red algae *Gracilaria chilensis* monitored in several sites (Vieira et al., 2018a,b). Here, we focus on how the probability of a frond being fecund (y) depends on its size (x) following a sigmoid-shaped curve. The raw data allowing determination of this probability included the observations of whether, at a given census, each frond was fecund (1) or not (0) depending on the logarithm of its frond volume (log(v), with v measured in cm^3). Generalized Linear Models (GLM) is the first method that comes to mind, using the logit link function and the Bernoulli distribution. Besides being the commonly proposed for binary data, the sigmoid shape of the resulting logistic regression fits the expectations for this data-set. However, posterior analysis revealed that the symmetrical s-shape of the logistic function misfits the data, with non-symmetrical alternatives as the Gompertz or the Weibull curves yielding better fits.

Sigmoid-shaped (or S-shaped) curves were developed and have traditionally been used to model mortality, survival and growth rates of populations, individuals and cells. The most commonly used are the Logistic, the Gompertz, the Weibull and the von Bertalanffy (Austin et al 2011, Paine et al., 2012; Tjørve and Tjørve, 2017). Their Sigmoid (or S) class name is due to their shape typically comprising an initial exponential increase that, beyond an inflexion point, is smoothed until leveling-off close to an asymptotic maximum.However, these curves do not necessarily show the sigmoid shape within the desired range for the independent variable. In this work we focus on the Gompertz and on the Weibull curves, both of which have been presented in a variety of forms. Most often, the Gompertz is written with three parameters (Gompertz, 1825; Winsor, 1932; Laird, 1964; Haefner, 1996; Pletcher, 1999; Jukic et al., 2004; Lynch and Fagan, 2009; Borah and Mahanta, 2013; Tjørve and Tjørve, 2017) whereas the Weibull is written with four (Dumur et al., 1990; Haefner, 1996; Lynch and Fagan, 2009; Mahanta and Borah, 2014). These versions have better shaping ability than their alternatives, enabling better fits to the data. Generally, parameter estimation is easier when minimizing the Sum of Squares of the Error (SSE) in linear regression, as it has a closed form i.e., an analytical solution. However, both the Gompertz and the Weibull curves can only be linearized by transformation or scaling assuming that at least one of the parameters is previously known (Winsor, 1932; Laird, 1964; Borah and Mahanta, 2013; Tjørve and Tjørve, 2017). Since this is usually not the case, the estimation of their parameters is substantially more difficulty. Alternatively, the parameters can be determined from Maximum Likelihood Estimates (MLE). Although argued that MLE provide better fits, narrower confidence intervals, and are more compatible with a posteriori tests (Pletcher, 1999), the most common option has beento use non-linear least-squares regressions(Laird, 1964; Jukic et al., 2004; Lynch and Fagan, 2009; Borah and Mahanta, 2013; Mahanta and Borah, 2014). In this case, the minimization of the SSE has no analytic solutionwith search algorithms being required. However, these methods are prone to the numerical instability (Bates and Watts, 1988; King and Mody, 2010; Lange, 2010), and their application to Sigmoid-shaped curves are among the most difficult (Jukic et al., 2004; Borah and Mahanta, 2013; Mahanta and Borah, 2014). The benchmark is the Newton-Raphson method, due to its speed of convergence to a solution (Bates and Watts, 1988; King and Mody, 2010; Lange, 2010; Mahanta and Borah, 2014). The algorithm of widest spread is the Gauss-Newton method(Bates and Watts, 1988; King and Mody, 2010; Lange, 2010; Weisstein, 2018), with its several updates - as the Levenberg-Marquardt algorithm - to solve for the frequent numerical instability by controlling the search's step size (Bates and Watts, 1988; King and Mody, 2010; Lange, 2010). One particular source of instability is the system of equations being ill-conditioned (Seber and Lee 2003; King and Mody, 2010; Vieira et al., 2016). A solution proposed to solve such type of instability is scaling the variables (Seber and Lee 2003; Vieira et al., 2016). Although some consider it a false solution that is unable to

resolve ill-conditioning problems (at least, theoretically) (King and Mody, 2010), it was observed to effectively solve them (Vieira et al., 2016). Here, we tested and compared several solutions to stabilize the calculus, as scaling the variables, setting approximate initial conditions, controlling the step-size of the search or using a positive definite matrix to re-direct it.

Most observations belonging to intermediate sizes is another common problem illustrated by this study (Fig.1): 4111 of the observations (90% of the sample) had frond volumes within 0.1 cm^3 and 200 cm^3, whereas only 460 of the observations (10% of the sample) had frond volumes beyond these bounds. The scarcity of observations in both size extremes undermined the fit and the confidence in the shape of the curve. To overcome this problem, it is proposed an alternative to GLM where the Gompertz and Weibull curves are estimated balancing the contribution of the different x classes (frond sizes, in this case) to the curve fitting process. If, on the one hand, this may improve the curve-fit, on the other hand, it introduces an uncertainty on the probabilities estimated for each size class when these have small numbers of individuals. As an example, within a size class comprising only three observations, each observation (of 0 or 1) represents a 0.33 change in the estimated probability. Such high uncertainty suggests that a minimum number of observations in each size class could be required to yield reliable fits. However, discarding size classes considered as presenting insufficient numbers of individuals may lead to the absence of data in the extreme parts of the curve that may be essential for its definition. In this work we compare the absence of data against data with poor quality.

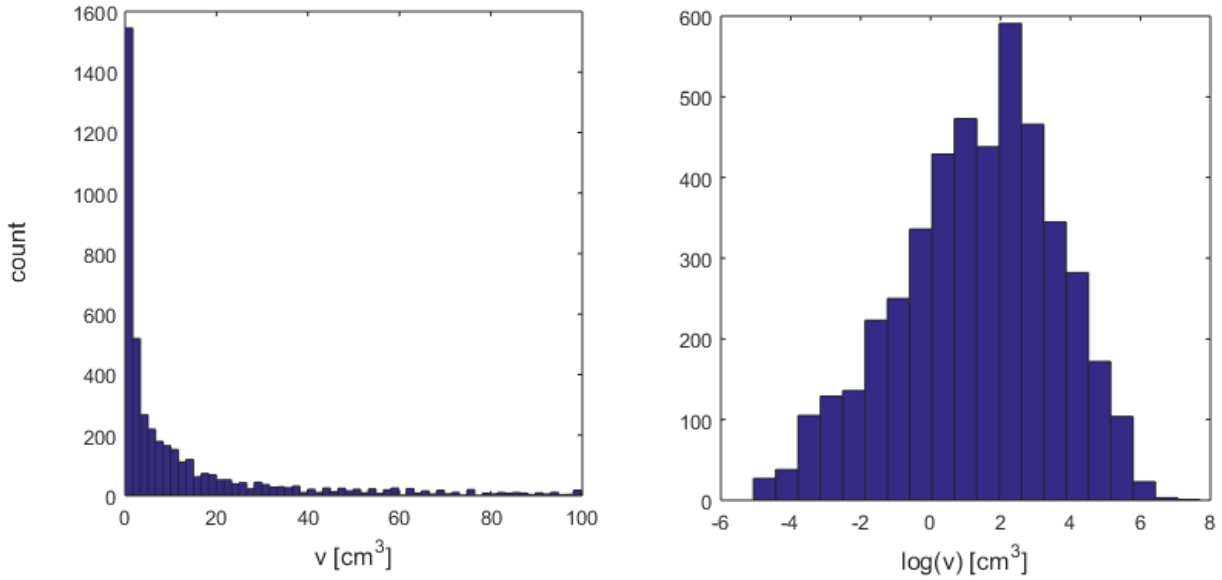

Fig. 1 Probability density functions of the dependent variable (predictor). The predictor frond volume (v) is presented in linear and logarithmic scales, with at least one of the tails of the respective distributions being scarce in observations.

Knowing that the common biologist and ecologist does not necessarily master numerical methods and programing tools, a software and guiding lines are provided that facilitate fitting Gompertz and Weibull curves to their binary data. The solutions estimate all parameters based only on observed data and not requiring that at least one of them is known *a priori*. Several options were tested and compared, namely:

(i) fitting the Gompertz vs the Weibull curves;

(ii) estimating the parameters minimizing the SSE *vs* maximizing the log-likelihood;

(iii) using the Newton-Raphson, Gauss-Newton or Levenberg-Marquardt search algorithms;
(iv) using several options to improve the performance of the search algorithms;
(v) grouping the data into x classes to improve the accuracy of the fits in the extremes of the curves.

2 Methods

2.1 Data

Gracilaria chilensis is a red macroalga with a typical isomorphic biphasic life-cycle alternating between diploid (tetrasporophytes) and dioecious haploid (male and female gametophytes) free living generations (Kamiya and Kawai, 2002; Guillemin et al., 2013; Vieira et al., 2018a,b). Individuals were monitored in five intertidal rock-pools in two sites (Corral 39°52'27"S / 73°24'02" W and Niebla 39°55'47"S / 73°23'57"W) within the Valdivia River estuary, from October 2009 to February 2011 at four-month intervals(Vieira et al., 2018a,b). All individuals were mapped relative to a pair of fixed points. At each census, the presence (1) or absence (0) of reproductive structures was recorded for each individual and used as observed response (y). Concomitantly, the volume of each individual was recorded and used as explanatory (independent) variable after transformation by x=ln(v). The probability of an individual being fecund (ρ) depending on its size (x) was estimated for each stage×site×season combination.

When individuals were grouped, nine size classes were used centered at x={-3, -1, 0, 1, 2, 3, 4, 5 and 7}. For each stage×site×season combination, the probability of an individual within a size class to be fecund (y) was determined by $y=n_f/n_t$, where n_f and n_t werethe counts of fecund individuals and of all individuals, respectively.

2.2 Software and analysis design

The SCurves1.m Matlab script fits one curve to a specific data-set using the original ungrouped observations. Alternatively, the SCurves2.m Matlab script fits one curve grouping the observations into x classes. The SCurves3.m Matlab script fits a curve for each combination of season, site and life cycle stage grouping the observations into x classes.

We show how to choose the options and fit the curves using the latter script as example. The script has an initial section for the 'Settings' where all options are defined. The ones relative to the data are:

i) Importing the data (in script line 10). It includes the path and the name of the file.
ii) Declaring the variables (in script lines 13 to 27). Variables #1 and #2 were for x and y, respectively. We only used the {x,ρ} pairs for which v>0. Variables #3 to #5 were for the categorical variables season, site and life-cycle stage.
iii) Defining the size classes by declaring their centers (in script line 30). Their edges are set automatically midway between adjacent size classes. The script automatically sets the smallest class as an open interval to -∞ and the largest class as an open interval to ∞.
iv) The minimum number of observations within a size class (n_{min}) for it to be used in the calculus (in script line 33). We compared the curves fitted using $n_{min}=1$ and $n_{min}=5$.

2.3 Sigmoid-shaped curves

The Gompertz curve estimated the probability (ρ) of an individual sized x=ln(v) to be fecund relying on three parameters: the asymptotic maximum (K_∞), the displacement of the curve along the x axis (b), and the increment rate (c) (Equation 1a). The Weibull function estimated the same relation from a slightly different structure with an extra parameter: the lower asymptote (K_0) (Equation 1b). However, the Weibull function does not accept x<0. In this example it implied that we could not use the Weibull function to estimate ρ for

individuals sized v<1 cm^3. The choice of the type of curve being fit was done in script line 39.

$$\rho = K_\infty \cdot e^{-b \cdot e^{-c \cdot x}} \quad (1a) \qquad \rho = K_\infty + \left(K_0 - K_\infty\right) \cdot e^{-(bx)^c} \quad (1b)$$

2.4 Scaling of x and y

Because scaling is alleged to stabilize optimization algorithms (Seber and Lee 2003; Vieira et al., 2016), both variables were optionally scaled so that $\dot{x}=x/x_M$ and $\dot{y}=y/y_M$, with x_M and y_M corresponding to the maximum observed values of x and y, respectively. Scaling or not the variables was chosen in script line 36. The application of the Gompertz and Weibull curves to the scaled variables led to the estimation of parameters specific to those scaled dimensions:

$$y = \dot{K}_\infty \cdot e^{-\dot{b} \cdot e^{-\dot{c} \cdot \dot{x}}} \quad (2a) \qquad y = \dot{K}_\infty + \left(\dot{K}_0 - \dot{K}_\infty\right) \cdot e^{-(\dot{b}\dot{x})^{\dot{c}}} \quad (2b)$$

A conversion between original and scaled related parameters was required: (i) prior to the search, to convert the initial guess in the form of original parameters into their scaled counterparts, and (ii) after the search, to convert the solutions in the form of scaled parameters into their original counterparts. This was done for the Gompertz curve by the system of equations (3a), and for the Weibull curve by the system of equations (3b).

$$\begin{cases} \dot{K}_\infty = \dfrac{K_\infty}{y_M} \\ \dot{b} = b \\ \dot{c} = c \cdot x_M \end{cases} \quad (3a) \qquad \begin{cases} \dot{K}_\infty = \dfrac{K_\infty}{y_M} \\ \dot{K}_0 = \dfrac{K_0}{y_M} \\ \dot{b} = b \cdot x_M \\ \dot{c} = c \end{cases} \quad (3b)$$

2.5 Non-linear least squares regression

The curve parameters, $\beta=\{K_\infty,b,c\}$ in the Gompertz case and $\beta=\{K_\infty, K_0,b,c\}$ in the Weibull case, were estimated by non-linear least squares regression. Because it has no closed form (i.e, analytical) solution, it required numerical estimation. Search methods were used to find the set of parameters (β) that minimized the Sum of Squares of the Error (SSE) (Equation 4):

$$\{K_\infty, K_0, b, c\} = \arg\min_{\beta} \sum \left(y - \rho\right)^2 \quad (4)$$

The search started with an initial set of parameters β_i that was iteratively updated by $\beta_{i+1}=\beta_i+\Delta\beta$ until the SSE stabilized in a minimum. The Newton-Raphson method, the Gauss-Newton method and the Levenberg-Marquardt algorithm diverged in the determination of $\Delta\beta$. The choice of search method was done in script line 42. To guarantee that stabilization occurred in the desired global minimum and not in a different local minimum, the initial β_i was already close enough from the solution (Bates and Watts, 1988; Jukic et al., 2004; King and Mody, 2010; Lange, 2010; Borah and Mahanta, 2013; Vieira et al., 2016). These initial conditions were defined in script lines 60 to 77. To aid choosing the initial β_i, when plotting the results, the script added a

dotted red line representing the initial curve. But even with good initial guesses, search algorithms were still prone to give steps (Δβ) too large, overshooting the solution (Bates and Watts, 1988; King and Mody, 2010; Lange, 2010; Borah and Mahanta, 2013). We adopted the most common and simplest solution of decreasing the step size by a factor, leading to $\Delta\beta_{new} = \Delta\beta \cdot$ shift-cut with 0≤shift-cut≤1. If this did not reduce the SSE, the $\Delta\beta_{new}$ was iteratively decrease by the same shift-cut until the SSE was reduced. The shift-cut value was set in script line 48. This strategy was only applied with the Newton-Raphson and the Gauss-Newton methods. More intricate strategies to decrease the Δβ exist, as is the case of the Levenberg-Marquardt algorithm.

The Gauss-Newton method solved the normal equations for Δβ(equation 5a). It required the residuals between observations and estimates (Δρ=y-ρ) and the Jacobian matrix (J) of the curve function in order to the k parameters given the j observations (i.e., $\partial\rho_j/\partial\beta_k$). The ρ, Δρ and J were updated during each iteration. Given the possibility that observations were not all equally important, the Δβ was also solved weighting the observations relative to their variance (equation 5b). In this case the weighting matrix W was the diagonal matrix of the reciprocal of the variance-covariance matrix of the observations i.e., $W=\text{diag}(\text{cov}(y_j)^{-1})$. The choice to weight the observations was done in script line 45.

$$\Delta\beta = \left(J' \cdot J\right)^{-1}\left(J'\right)\left(\Delta\rho\right) \qquad (5a)$$

$$\Delta\beta = \left(J' \cdot W \cdot J\right)^{-1}\left(J' \cdot W\right)\left(\Delta\rho\right) \qquad (5b)$$

The Jacobian matrix (J) of the Gompertz curve considering the observations j={1,2,…, j} was given by Appendix equation (Ia), with its matrix entries given in Appendix equations (Ib-Id). The Jacobian matrix (J) of the Weibull curve considering the observations j={1,2,…, j} was given by Appendix equation (IIa), with its matrix entries in equations (IIb-IIe).

The Levenberg-Marquardt algorithm improved the convergence ability of the Gauss-Newton method by implementing its damped versions, with the cost of increased calculus (Levenberg, 1944; Marquardt, 1963). The standard search was done by equation (6a) whereas the weighted search by equation (6b). The diagonal of J'J scaled the components of the search according to the curvature, thus increasing the step-size along the directions with small gradients. This method included a primary (parent) search for Δβ within which was executed a secondary (child) search for the damping factor λ. Within the child search, an initial damping factor λ_0 was set to a value slightly above 1 (in script line 51). The effective damping factor $\lambda=\lambda_0.v^{lm}$ was iteratively estimated setting v to a value slightly above 1 (in script line 54) and testing lm=-1 to lm=7. We started by lm=-1, fit the curve and then compared the new SSE to the old SSE. If no improvement in the curvefit was observed, lm was iteratively increased by 1, a new curve was fit, and the SSE updated. If the fit was improved before lm>7 the child search stopped and the parent search progressed to the next iteration. But if there was no improvement even when lm=7, the whole method (i.e., both searches) stopped and the current β was assumed as the final solution.

$$\Delta\beta = \left(J' \cdot J + \lambda \cdot diag\left(J'J\right)\right)^{-1}\left(J'\right)\left(\Delta\rho\right) \qquad (6a)$$

$$\Delta\beta = \left(J' \cdot W \cdot J + \lambda \cdot diag\left(J'J\right)\right)^{-1}\left(J' \cdot W\right)\left(\Delta\rho\right) \qquad (6b)$$

When β minimized the SSE the derivative $\partial SSE/\partial\beta=0$. The Newton-Raphson method converged to its roots

iteratively estimating $\Delta\beta=-J^{-1}u$, where $u=\partial SSE/\partial\beta$ and $J=\partial^2 SSE/\partial\beta^2$ (King and Mody, 2010, Lange 2010, Mahanta and Borah, 2014). When using the Gompertz curve, u assumed the form in Appendix equation (IIIa) with the partial derivatives corresponding to Appendix equations (Ib-Id), while J assumed the form in Appendix equations (IIIb) with partial derivatives given by Appendix equations (IIIc-IIIh). When using the Weibull curve, u assumed the form in Appendix equation (IVa) with partial derivatives given by Appendix equations (IIb-IIe), while J assumed the form in Appendix equation (IVb) with partial derivatives given by Appendix equations (IVc-IVl). Far from the solution, this method is equally happy to converge or diverge its search. Forcing it to converge can be achieved replacing J by a positive definite matrix (Lange, 2010). We used the identity matrix.

2.6 Maximum Likelihood Estimation (MLE)

The curve parameters, $\beta=\{K_\infty,b,c\}$ in the Gompertz case and $\beta=\{K_\infty, K_0,b,c\}$ in the Weibull case, were estimated by Maximum Likelihood applied to the ungrouped observations. Given a set of identical independently distributed (idd) observations $y=\{y_1,y_2,\ldots,y_n\}$, their likelihood was given by $L(\rho;y)$ (equation 7). However, in this case it was more convenient to work with the log-likelihood $\ell(\rho;y)$ (equation 8).

$$L(\rho;y)=\prod^{n} f(y_i\mid\rho) \qquad (7)$$

$$\ell(\rho;y)=\frac{1}{n}\sum^{n}\ln\left(f(y_i\mid\rho)\right) \qquad (8)$$

The ρ was the probability of drawing y=1 input into the Bernoulli distribution (equation 9) along with the y observations (0 or 1).Usually, the Bernoulli distribution refers to p. However, to avoid confusion with the significance p, throughout this article it was replaced by ρ. In the simplest case, ρ is a constant estimated from the maximum log-likelihood, i.e., ρ assumes the value that maximizes the log-likelihood (equation 10).The ρ value maximizing the log-likelihood can even be searched and found manually, which is a good exercise to understand and practice this method. However, this case was more complicated since ρ was not a constant but a variable dependent from ln(v) following the Gompertz (equation 1a) or the Weibull (equation 1b) curves. Hence, it was required to find the K_{inf}, K_0, b and c values yielding the ρ that maximized the log-likelihood (equation 11).

$$f(y_i\mid\rho)=\rho^{y_i}(1-\rho)^{1-y_i} \qquad (9)$$

$$\rho=\arg\max_{\rho}\ell(\rho;y) \qquad (10)$$

$$\{K_{\inf},K_0,b,c\}=\arg\max_{\rho}\ell(\rho;y) \qquad (11)$$

When $\beta=\{K_{inf},K_0,b,c\}$ maximized ℓ, the derivative $\partial\ell/\partial\beta=0$. The Newton-Raphson method iteratively converged to its roots applying $\beta_{t+1}=\beta_t+\Delta\beta$ and estimating $\Delta\beta=-J^{-1}u$ (King and Mody, 2010, Lange 2010), where $u=\partial\ell/\partial\beta$ and $J=\partial^2\ell/\partial\beta^2$. When using the Gompertz curve, u assumed the form in Appendix equation (Va), with first order partial derivatives given by Appendix equations (Ib-Id), while J assumed the form in

equations (Vb and Vc) with first order partial derivatives given by Appendix equations(Ib-Id)and second order partial derivatives given by Appendix equations (Vd-Vi). When using the Weibull curve, u assumed the form in equation (VIa), requiring the first order partial derivatives presented in equations (IIb-IIe), while J assumed the form in equations (VIb and Vc) requiring the first order partial derivatives (equations IIb-IIe) together with the second order partial derivatives presented in equations (VIc-VIh):

Alternatively to MLE using the Newton-Raphson method, the MLE using the Matlab embeded fmincon function provided in its Optimization Toolbox, was also tested. Since this is a multidimensional optimization problem, the application of the fmincon function is not as straight-forward as in Matlab's tutorial. The programming sequence used is presented hereafter. Prior to the calculations, it was defined a custom @myfun function to be invoked during calculations. For the Gompertz curve it was created the Gompertz_MLE.com script with the code lines:

```
function l = Gompertz_MLE(x,y,n,beta)
Kinf = beta(1);
b    = beta(2);
c    = beta(3);
yest = Kinf.*exp(-b.*exp(-c*x));
fBer = yest.^y.*(1-yest).^(1-y);
l    = -1/n*sum(log(fBer));
```

This script yields the -ℓ of the Gompertz curve given $\beta=\{K_\infty,b,c\}$ and assuming that the observations follow a Bernoulli distribution. The -ℓ was used because it was wished to find the β maximizing ℓ but the fmincon is a minimization algorithm. The adaptation to the Weibull curve required introducing an extra line for K_0, adapting β for K_0 and replacing for the Weibull equation in the 'yest' line. The next step was running the Scurves1.m script until line 83 with the objectives of (i) selecting the explanatory (x) and response (y) variables, (ii) defining the sample size (n), (iii) selecting the stage×month×pool combination to test, and (iv) defining the initial K_∞, b and c parameters. Then, defining the fmincon options was required. Its Active-Set search algorithm was the only consistently providing solutions to the optimization problem. Hence, in Matlab's command window was typed:

```
options=optimset('Algorithm','active-set','MaxFunEvals',1000);
```

Although it was chosen admitting up to 1000 iterations, the algorithm usually converged in less than 20. The fmincon function could finally be run typing in the command window:

```
[beta,~,~,~]=fmincon(@(beta)Gompertz_MLE(x,y,n,beta),beta,[],[],[],[],[],[],[],options);
Kinf          = beta(1);
b             = beta(2);
c             = beta(3);
```

This particular fmincon syntax states that the -ℓ is minimized searching the optimal β and not the x, y or n, without constrains for equalities or inequalities, and without upper and/or lower boundaries.

3 Results and Discussion

When the curves were estimated from the original (ungrouped) observations, 126 to 458 observations were comprised within each stage×month×pool combination. These large sample sizes were fundamental for the stability of the SSE minimization, leading all search algorithms to always converge into similar curves. The strategies used to stabilize the searches were of little relevance and the searches were little sensitive to the initial conditions. On the contrary, when the curves were estimated from MLE the calculus was often unstable. The Newton-Raphson method was unable to find the MLE solution for 2 out of the 18 stage×month×pool combinations, while the Matlab embedded fmincon function was unable to find the MLE solution for 4 combinations. When the curves were estimated from grouped observations, 5 to 9 groups were comprised within each stage×month×pool combination, with the calculus becoming highly unstable. Hence, the first task was tuning the search algorithms. Only afterwards could the grouped binary data be tested with confidence.

As commonly happens with Sigmoid-shaped functions, the Gompertz and Weibull equations used in this study had intricate structures that easily pointed the optimization algorithms to search in the wrong direction or to overshoot the solution. Hence, providing good initial guesses for the curve parameters is a key aspect in the application of search algorithms (Jukic et al., 2004; King and Mody, 2010; Lange, 2010; Oswald et al., 2012). When applying the grouping method, good initial guesses could always be obtained from a former parameter estimation from ungrouped observations.

When using the Newton-Raphson method to estimate the Gompertz curve parameters the searches easily started drifting erratically. Hence, this method was only useful after stabilization, which required the simultaneous use of (i) a positive definite matrix preventing the search to move in the wrong direction, and (ii) a shift-cut ≤0.46preventing the search to over-shoot the solution. When these two options were simultaneously applied, the search converged to adequate solutions (Figs 2 and 3). In these cases, scaling the variables was useless and often had a deleterious effect. The numerical instability was more severe when the Newton-Raphson method was applied to the Weibull curve. Then, obtaining good fits for all curves required 0.1≤ shift-cut ≤0.2.In rare occasions it was better to scale the variables, but usually this option was irrelevant. Despite all the difficulties, the Newton-Raphson method was the only able to fit Weibull curves on a regular basis and with a single tuning.

When the Gauss-Newton method converged, it was exactly to the same solutions as the Newton-Raphson method (Fig. 3). However, the Gauss-Newton method was the most unstable of them all, the reason why it was the least preferred for this dataset. Either applied to estimate the Gompertz or the Weibull curves, convergence required initial guesses very close to the final solution. Using the same initial guesses as in the previous test with the Newton-Raphson, and it was impossible to fit all curves i.e., whatever the tuning, there were always a few curves for which the search did not converge. Scaling the variables or weighting the observations was useless.

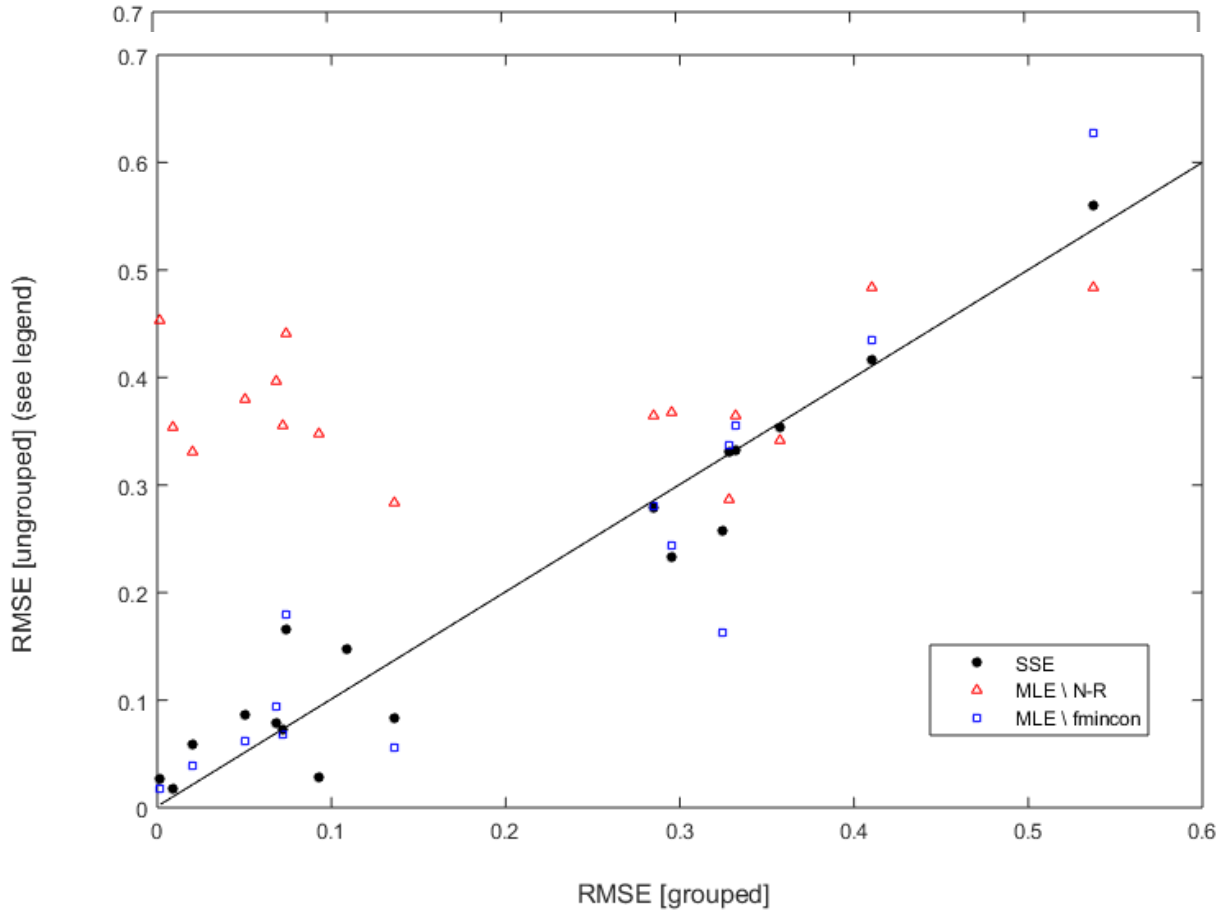

Fig. 2 Tuning the Newton-Raphson method to fit the Gompertz curve. The accuracy of the fits are given by the Root Mean Square Error (RMSE), with the searched method using a positive definite matrix and a shift-cut (a: in x axis), or without using a positive definite matrix and a shift-cut (b: in y axis). The solid grey line is the 1:1 line. The effect of scaling or not both variables is also shown. All fits started from reasonably close initial guesses.

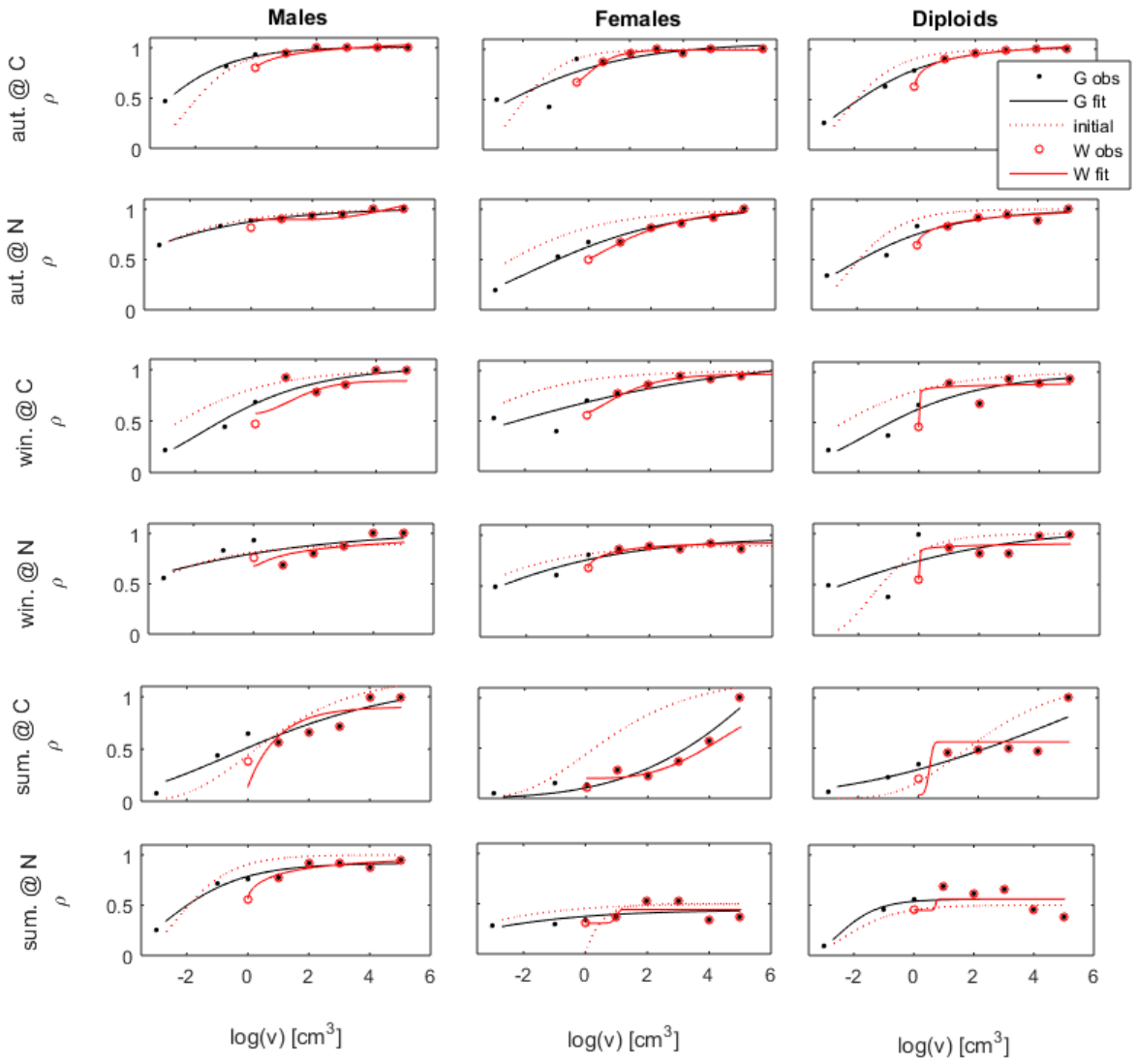

Fig. 3 Comparing sigmoid curves. Observations and estimates for the (ρ) probability of fronds with (v) volume being fecund. Curvefits split among life-cycle stages Males, Females and Diploids, seasons Autumn (aut), Winter (win), and Summer (sum), and sites Corral (C) and Niebla (N)., and using all size classes with at least one observation. The observations (G obs) were used to fit the Gompertz curve (G fit) by any of the methods with the search starting from initial guesses (initial). The observations (W obs) were used to fit the Weibull curve (W fit) by the Newton-Raphson method.

The Levenberg-Marquardt algorithm was the most stable and easiest to apply with the Gompertz curve. Tuning it to $0.1 \leq \lambda \leq 5$ and $1 < v < 3$ led the searches to always converge, fitting curves identical to the ones provided by the Newton-Raphson method and the Gauss-Newton method at their finest performance (Fig. 3). Therefore, it was the favorite method for fitting the Gompertz curve. This was expectable as the Levenberg-Marquardt was the last of these methods to be developed, and precisely aiming to solve the stability issues of its predecessors (Levenberg, 1944; Marquardt, 1963). However, when fitting the Weibull curve, things changed drastically. There was no effective tuning of the Levenberg-Marquardt algorithm leading all searches to converge. A few curves were always left unfit. Again, scaling the variables or weighting the observations was useless, both for fitting the Gompertz or the Weibull curves. From all these tests was concluded that there is no overall better method. Their performances change with the data properties and the curve being fit

(Levenberg, 1944; Marquardt, 1963; Bates and Watts, 1988; Jukic et al., 2004; King and Mody, 2010; Lange, 2010; Borah and Mahanta, 2013).

The threshold number of observations within a class for itto be accepted in the 'grouping the data' method was tested comparing between using all classes with at least one or with at least five observations. For this test, Gompertz curves were fit applying the Levenberg-Marquardt algorithm. In 11out of the 18 curves, both thresholds made no difference (Fig.4). In five of the cases where using a n≥5 threshold eliminated size classes, this made no (or little) difference for the curve-fits. In these cases, also using the size classes with n<5 confirmed the adequacy of the curve-fit for a wider range of the explanatory x variable, and thus conferred more confidence on these fits. In the remaining two cases, using less classes decreased the quality of the fits, leading to conspicuously different and less credible curves. Our tests suggest that it is preferable to use the largest quantity of data (i.e., x classes) possible, even if the quality of the extra data is lower (i.e., there is less confidence on the y averaged for these x classes). Nonetheless, these are only preliminary results and more extensive testing is required.

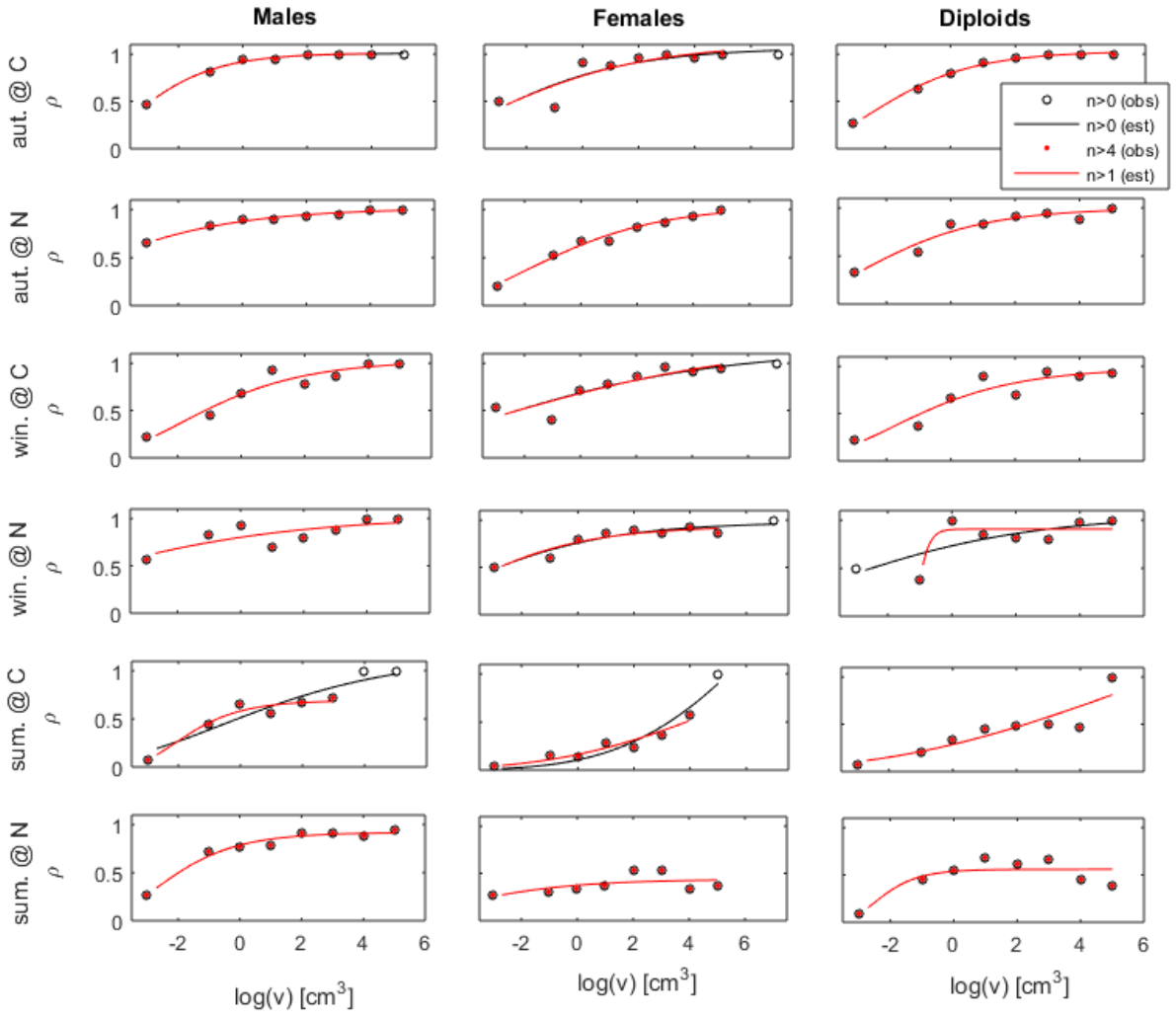

Fig. 4 Data quantity vs quality.Gompertz curves were fit by the Levenberg-Marquardt algorithm using size classes with at least one observation (n>0) or just the size classes with at least 5 observations (n>4). Where the black lines are not visible it is because they are covered behind by the red curves. Values (obs) observed and (est) estimated for the (ρ) probability of fronds with (v) volume being fecund. Curvefits split among life-cycle stages Males, Females and Diploids, seasons Autumn (aut), Winter (win), and Summer (sum), and sites Corral (C) and Niebla (N).

The estimation of Gompertz curves from observations grouped into size classes was compared against their estimation directly from the original ungrouped observations, either by minimizing the SSE or maximizing the log-likelihood. For many of the stage×month×pool combinations, both 'grouped' and 'ungrouped' methods yielded resembling curves (Fig.5). In these cases, the advantage of grouping observations is only the visual effect of the plots. The remarkable visual fits between lines and size class averages are intuitively accepted. On the contrary, the exact same lines are intuitively questioned when plotted against raw observations that are either 0 or 1, despite in both cases the supporting raw data being exactly the same. In the stage×month×pool combinations where the 'grouped' and 'ungrouped' methods yielded conspicuously different curves, these diverged mainly in their extremes (Fig. 5), which is precisely where the application of the 'grouped' method is expected to be advantageous. While in the center of the curves, where the bulk of the observations are, the 'ungrouped' method should provide better fits because the searches provided the parameters optimizing the fits to this bulk; in the curves' extremes the 'grouping' method, by enhancing the weights of the observations therein, should generally provide better fits. To tests the accuracy of the fits specifically in these extremes we estimated the root mean square deviation (RMSE) using only observations of fronds smaller than 0.02 cm^3 or larger than 200 cm^3 (Fig. 6). Comparing to the ungrouped- SSE method, in 10 out of the 18 stage×month×pool combinations the 'grouped' method provided better fits (i.e., smaller RMSE), and only in 4 cases was it the other way around. This contrast was even more stringent when comparing to the ungrouped- MLE methods, and we recall that these latter were even unable to find the solutions for several curve-fits. Maybe in most applications of the Gompertz and Weibull curves is more important to focus on the accuracy of the curves at their centers, where the bulk observations are. In such cases, not grouping the observations seems as good a choice as grouping them. However, there are applications where the most important is to have curves that are accurate at their extremes despite the reduced number of observations therein. In such cases, grouping the observations will likely provide better curve-fits.

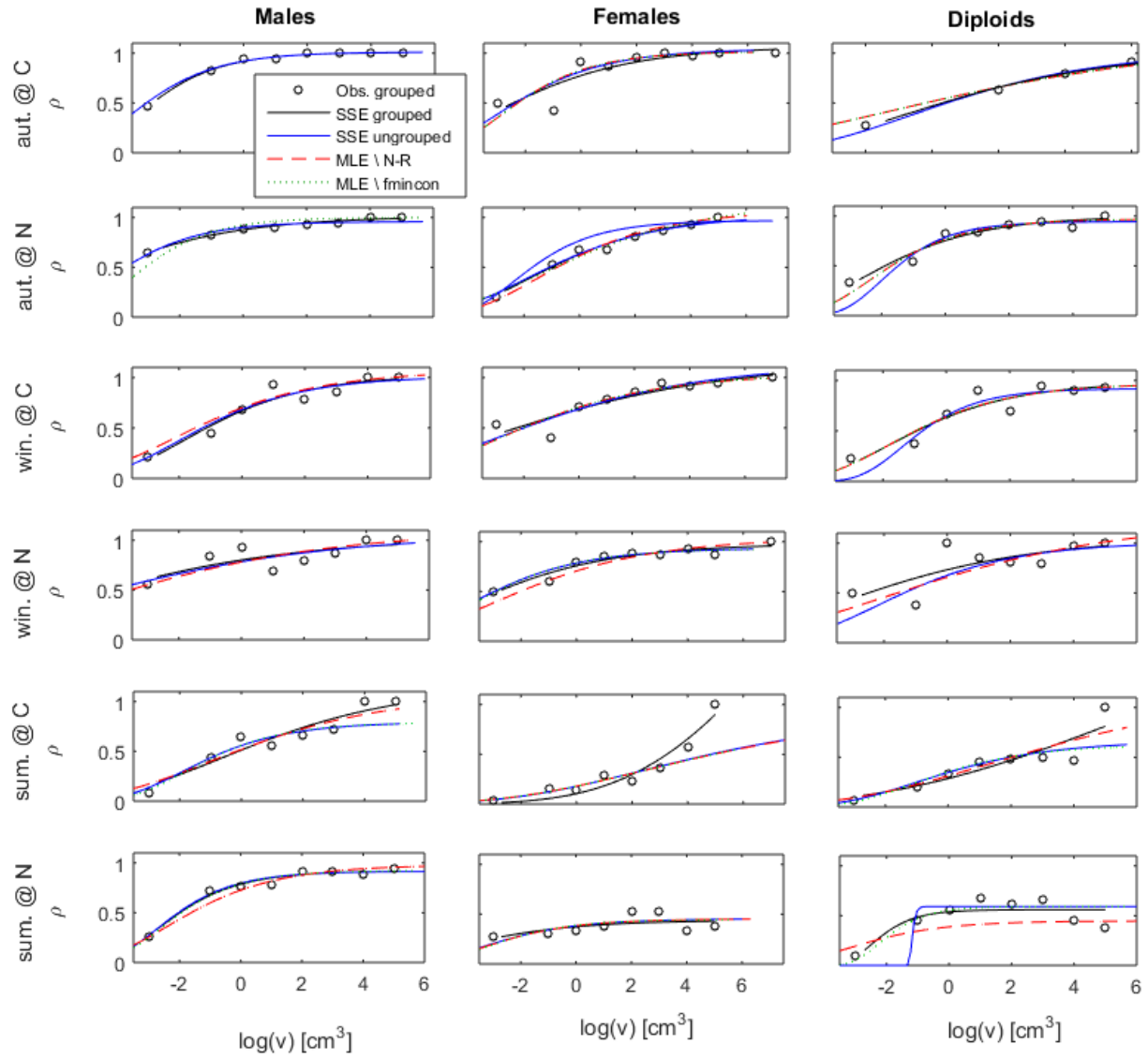

Fig. 5 Curve fits of grouped vs ungrouped observations, and SSE vs MLE. The probability (ρ) of individuals being fecund was dependent on their frond volume following a Gompertz curve. Curvefits split among life-cycle stages Males, Females and Diploids, seasons Autumn (aut), Winter (win), and Summer (sum), and sites Corral (C) and Niebla (N). The parameters were estimated by non-linear regression minimizing the error sum of squares using the Levenberg-Marquardt algorithm (SSE), by maximum likelihood estimation using the Newton-Raphson method (MLE \ N-R) and by maximum likelihood estimation using Matlab's fmincon function with the Active-Set algorithm (MLE \ fmincon). The parameters were estimated from the original observations (ungrouped) or the observations grouped into size classes (grouped). The MLE was always applied with ungrouped observations.

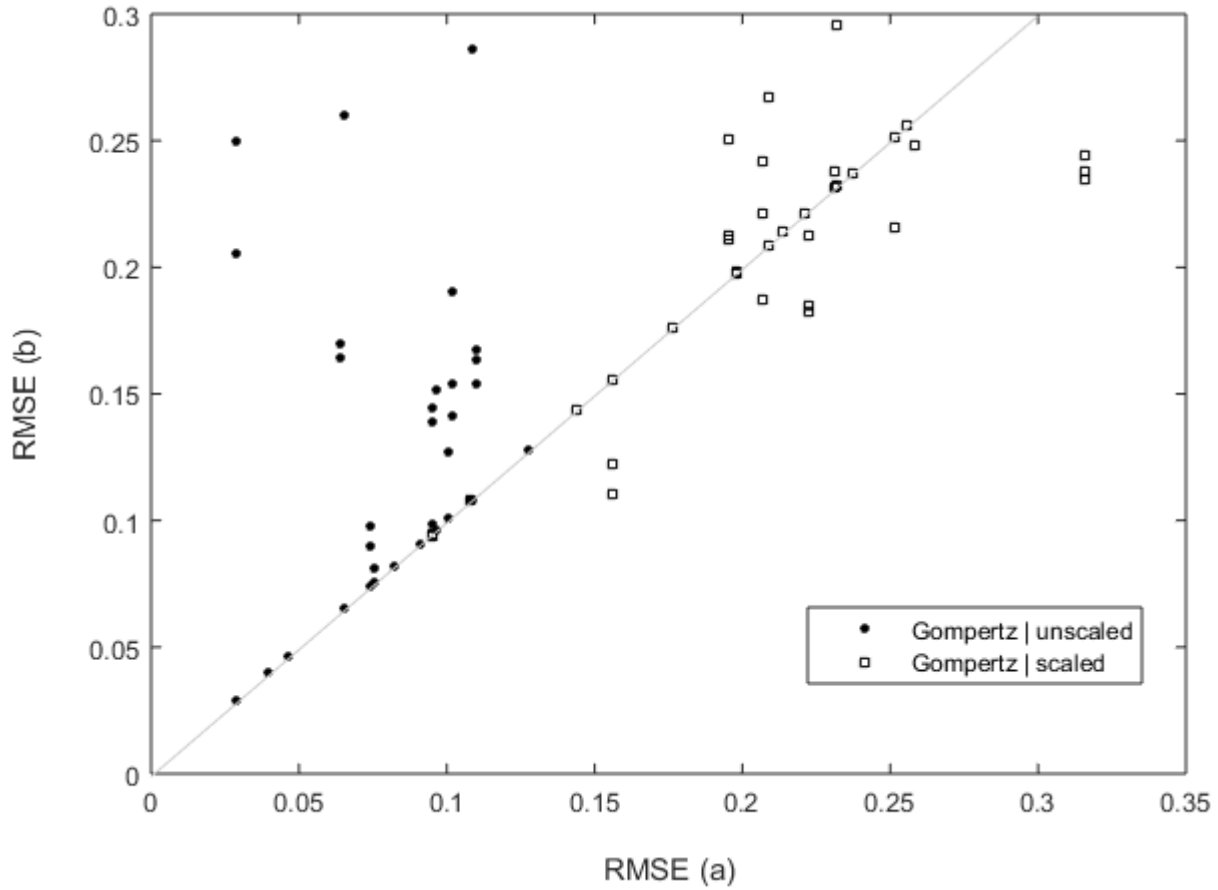

Fig. 6 RMSE of grouped *vs* ungrouped observations, and SSE vs MLE. Root Mean Square Deviation (RMSE) of the Gompertz curves fit grouping and not grouping the observations, and minimizing the SSE or maximizing log-likelihood.

In biological, ecological and evolutionary research it is fundamental to accurately fit non-linear growth, survival and fecundity(Austin et al., 2011; Oswald et al., 2012; Paine et al., 2012; Barbour et al., 2013; Wilson et al., 2017; Rosenbaum and Rall, 2018). This case study is an example of when the accuracy of the fit at the curve extremes is of paramount importance: the fecundity of *Gracilaria chilensis* was approximately constant per unit frond volume, resulting in a strong allometric relation between spore production and frond length. Hence, despite the bulk of the observation being of intermediate-size fronds, the bulk of the spores were produced by the few larger fronds (Vieira et al., 2018b). Exceptionally large fronds occurred even among stands dominated by small fronds (Vieira et al., 2016). Under these circumstances, the focus was on accurately estimating the probability of larger fronds to be fecund, while the accuracy of this estimate for the intermediate-sized fronds was of lesser relevance. We illustrate it with the estimation of carpospores produced by females at Corral during the summer of 2010. The fecund females produced an average of 21.3 spores per cm^3 of thallus; which was multiplied by the volume of each thallus and by its probability of being fecund to obtain the likeliest carpospore production (Fig. 7). Because most of the carpospores were produced by the few larger female fronds, the estimated overall carpospore production was highly dependent on the method used to estimate the probability (ρ) of a female to be fecund. In fact, the difference between the likeliest carpospore production by the single biggest female frond depending on the ρ curve used, was larger than the likeliest carpospore production by all the other female fronds pooled together.

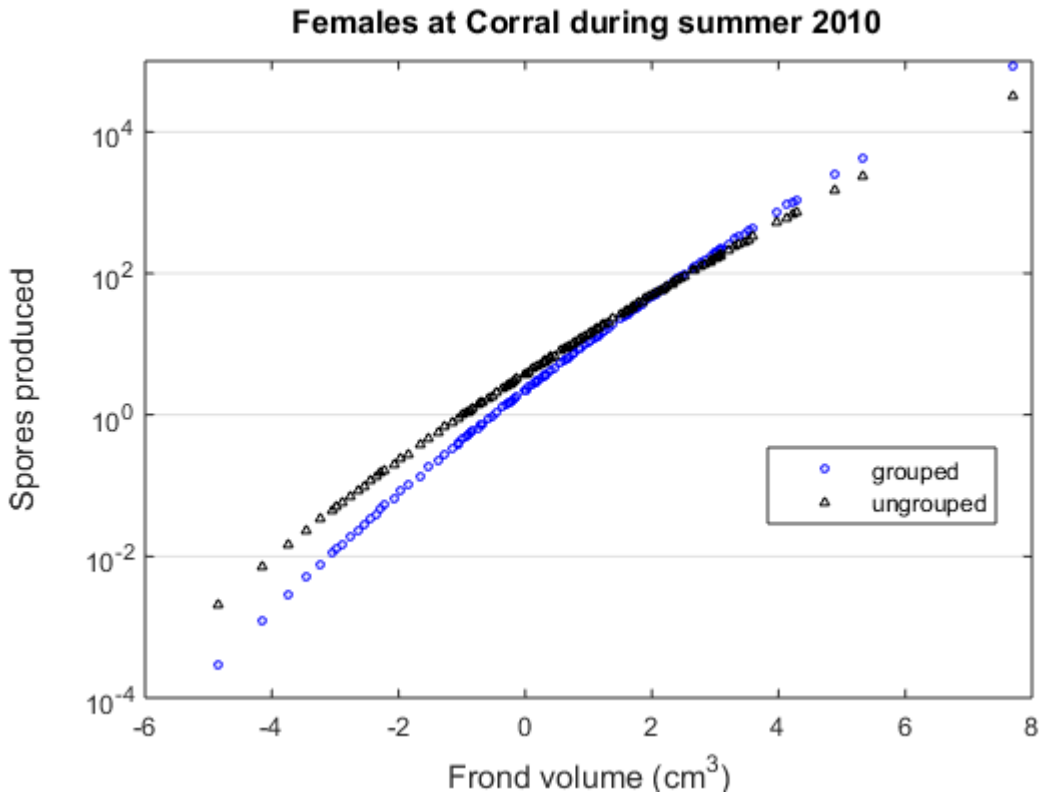

Fig. 7 Likeliest fecundity by size-class. The likeliest quantity of spores produced by each female monitored at Corral during the summer was dependent on the volume of its frond. This estimated spore production differed with the method (grouped vs ungrouped) used to estimate the probability of a frond to be fecund.

For many of the cases of larger size classes, our fits estimated $K_\infty>1$, implying probabilities >1, which is apparently incoherent. However, in practical terms, this is meaningless as it simply implies that individuals of those sizes are always fecund. We illustrate with the stochasticity of Individual Based Models: when applying these models, we simulate the fate of individuals one-by-one, and one-by-one we determine whether the individual is going or not to be fecund by randomly drawing a number between 0 and 1. If this number $<K_\infty$ the individual is going to be fecund, otherwise, is not. In practical terms, when individuals of a certain category are always fecund, it is irrelevant whether K_∞ is exactly 1 or how much larger than 1.In several stage×month×pool combinations the ρ did not show a leveling-off trend with increasing size (Figs 3-5). The most conspicuous cases were those of the females and diploids at Corral during the summer. In these cases, a $K_\infty>1$ was fundamental for the generation of curves accurately fitting the observations.

Appendix

$$J=\begin{bmatrix} \frac{\partial \rho_1}{\partial K_\infty} & \frac{\partial \rho_1}{\partial b} & \frac{\partial \rho_1}{\partial c} \\ \frac{\partial \rho_2}{\partial K_\infty} & \frac{\partial \rho_2}{\partial b} & \frac{\partial \rho_2}{\partial c} \\ \cdots & \cdots & \\ \frac{\partial \rho_j}{\partial K_\infty} & \frac{\partial \rho_j}{\partial b} & \frac{\partial \rho_j}{\partial c} \end{bmatrix} \tag{Ia}$$

$$\frac{\partial \rho}{\partial K_\infty}=e^{-b\cdot e^{-cx}} \tag{Ib}$$

$$\frac{\partial \rho}{\partial b}=-K_\infty e^{-cx-b\cdot e^{-cx}} \tag{Ic}$$

$$\frac{\partial \rho}{\partial c}=K_\infty bxe^{-cx-be^{-cx}} \tag{Id}$$

$$J=\begin{bmatrix} \frac{\partial \rho_1}{\partial K_\infty} & \frac{\partial \rho_1}{\partial K_0} & \frac{\partial \rho_1}{\partial b} & \frac{\partial \rho_1}{\partial c} \\ \frac{\partial \rho_2}{\partial K_\infty} & \frac{\partial \rho_2}{\partial K_0} & \frac{\partial \rho_2}{\partial b} & \frac{\partial \rho_2}{\partial c} \\ \cdots & \cdots & \cdots & \cdots \\ \frac{\partial \rho_j}{\partial K_\infty} & \frac{\partial \rho_j}{\partial K_0} & \frac{\partial \rho_j}{\partial b} & \frac{\partial \rho_j}{\partial c} \end{bmatrix} \tag{IIa}$$

$$\frac{\partial \rho}{\partial K_\infty}=1-e^{-(bx)^c} \tag{IIb}$$

$$\frac{\partial \rho}{\partial K_0}=e^{-(bx)^c} \tag{IIc}$$

$$\frac{\partial \rho}{\partial b} = -\left(K_\infty - K_0\right) e^{-(bx)^c} \cdot (bx)^{c-1} \cdot cx \tag{IId}$$

$$\frac{\partial \rho}{\partial c} = -\left(K_\infty - K_0\right) e^{-(bx)^c} (bx)^c \cdot \ln(bx) \tag{IIe}$$

$$u = -2\begin{Bmatrix} \sum_{i=1}^{n}\left(y_i - \rho_i\right)\frac{\partial \rho_i}{\partial K_\infty} \\ \sum_{i=1}^{n}\left(y_i - \rho_i\right)\frac{\partial \rho_i}{\partial b} \\ \sum_{i=1}^{n}\left(y_i - \rho_i\right)\frac{\partial \rho_i}{\partial c} \end{Bmatrix} \tag{IIIa}$$

$$J = \begin{Bmatrix} \frac{\partial^2 SSE}{\partial K_\infty^2} & \frac{\partial^2 SSE}{\partial K_\infty \partial b} & \frac{\partial^2 SSE}{\partial K_\infty \partial c} \\ \frac{\partial^2 SSE}{\partial b \partial K_\infty} & \frac{\partial^2 SSE}{\partial b^2} & \frac{\partial^2 SSE}{\partial b \partial c} \\ \frac{\partial^2 SSE}{\partial c \partial K_\infty} & \frac{\partial^2 SSE}{\partial c \partial b} & \frac{\partial^2 SSE}{\partial c^2} \end{Bmatrix} \tag{IIIb}$$

$$\frac{\partial^2 SSE}{\partial K_\infty^2} = 2\sum e^{-2be^{-cx}} \tag{IIIc}$$

$$\frac{\partial^2 SSE}{\partial K_\infty \partial b} = 2\sum\left(ye^{-cx-be^{-cx}} - 2K_\infty e^{-cx-2be^{-cx}}\right) \tag{IIId}$$

$$\frac{\partial^2 SSE}{\partial K_\infty \partial c} = -2b\sum\left(yxe^{-cx-be^{-cx}} - 2K_\infty xe^{-cx-2be^{-cx}}\right) \tag{IIIe}$$

$$\frac{\partial^2 SSE}{\partial b^2} = -2\sum\left(yK_\infty e^{-2cx-be^{-cx}} - 2K_\infty^2 e^{-2cx-2be^{-cx}}\right) \tag{IIIf}$$

$$\frac{\partial^2 SSE}{\partial b \partial c} = 2\sum\left(yK_\infty e^{-cx-be^{-cx}} x^2\left(be^{-cx} - 1\right) + K_\infty^2 e^{-cx-2be^{-cx}} x^2\left(2be^{-cx} - 1\right)\right) \tag{IIIg}$$

$$\frac{\partial^2 SSE}{\partial c^2} = -2K_\infty b\sum\left(ye^{-cx-be^{-cx}}x^2\left(be^{-cx}-1\right)-K_\infty e^{-cx-2be^{-cx}}x^2\left(2be^{-cx}-1\right)\right) \quad \text{(IIIh)}$$

$$u = -2\begin{Bmatrix}\sum_{i=1}^{n}(y_i-\rho_i)\frac{\partial\rho_i}{\partial K_\infty}\\ \sum_{i=1}^{n}(y_i-\rho_i)\frac{\partial\rho_i}{\partial K_0}\\ \sum_{i=1}^{n}(y_i-\rho_i)\frac{\partial\rho_i}{\partial b}\\ \sum_{i=1}^{n}(y_i-\rho_i)\frac{\partial\rho_i}{\partial c}\end{Bmatrix} \quad \text{(IVa)}$$

$$J = \begin{bmatrix}\frac{\partial^2 SSE}{\partial K_\infty^2} & \frac{\partial^2 SSE}{\partial K_\infty \partial K_0} & \frac{\partial^2 SSE}{\partial K_\infty \partial b} & \frac{\partial^2 SSE}{\partial K_\infty \partial c}\\ \frac{\partial^2 SSE}{\partial K_0 \partial K_\infty} & \frac{\partial^2 SSE}{\partial K_0^2} & \frac{\partial^2 SSE}{\partial K_0 \partial b} & \frac{\partial^2 SSE}{\partial K_0 \partial c}\\ \frac{\partial^2 SSE}{\partial b \partial K_\infty} & \frac{\partial^2 SSE}{\partial b \partial K_0} & \frac{\partial^2 SSE}{\partial b^2} & \frac{\partial^2 SSE}{\partial b \partial c}\\ \frac{\partial^2 SSE}{\partial c \partial K_\infty} & \frac{\partial^2 SSE}{\partial c \partial K_0} & \frac{\partial^2 SSE}{\partial c \partial b} & \frac{\partial^2 SSE}{\partial c^2}\end{bmatrix} \quad \text{(IVb)}$$

$$\frac{\partial^2 SSE}{\partial K_\infty^2} = 2\sum\left(1-e^{-(bx)^c}\right)^2 \quad \text{(IVc)}$$

$$\frac{\partial^2 SSE}{\partial K_\infty \partial K_0} = 2\sum\left(1-e^{-(bx)^c}\right)e^{-(bx)^c} \quad \text{(IVd)}$$

$$\frac{\partial^2 SSE}{\partial K_\infty \partial b} = -2\sum\left(1-e^{-(bx)^c}\right)(K_0-K_\infty)e^{-(bx)^c}\cdot(bx)^{c-1}\cdot cx \quad \text{(IVe)}$$

$$\frac{\partial^2 SSE}{\partial K_\infty \partial c} = -2\sum\left(1-e^{-(bx)^c}\right)(K_0-K_\infty)e^{-(bx)^c}\cdot(bx)^c\cdot\ln(bx) \quad \text{(IVf)}$$

$$\frac{\partial^2 SSE}{\partial K_0^2} = 2\sum e^{-2(bx)^c} \tag{IVg}$$

$$\frac{\partial^2 SSE}{\partial K_0 \partial b} = -2\sum \left(K_0 - K_\infty\right) e^{-2(bx)^c} \cdot (bx)^{c-1} \cdot cx \tag{IVh}$$

$$\frac{\partial^2 SSE}{\partial K_0 \partial c} = -2\sum \left(K_0 - K_\infty\right) e^{-2(bx)^c} \cdot (bx)^c \cdot \ln(bx) \tag{IVi}$$

$$\frac{\partial^2 SSE}{\partial b^2} = 2\sum e^{-2(bx)^c} \tag{IVj}$$

$$\frac{\partial^2 SSE}{\partial b \partial c} = 2\sum \left(K_0 - K_\infty\right)^2 e^{-2(bx)^c} \cdot (bx)^{c(c-1)} \cdot \ln(bx) cx \tag{IVk}$$

$$\frac{\partial^2 SSE}{\partial c^2} = 2\sum \left(\left(K_0 - K_\infty\right) e^{-(bx)^c} \cdot (bx)^c \cdot \ln(bx) \right)^2 \tag{IVl}$$

$$u = \frac{1}{n} \begin{Bmatrix} \sum_{i=1}^{n} \left(\frac{y_i}{\rho_i} - \frac{1-y_i}{1-\rho_i} \right) \frac{\partial \rho_i}{\partial K_\infty} \\ \sum_{i=1}^{n} \left(\frac{y_i}{\rho_i} - \frac{1-y_i}{1-\rho_i} \right) \frac{\partial \rho_i}{\partial b} \\ \sum_{i=1}^{n} \left(\frac{y_i}{\rho_i} - \frac{1-y_i}{1-\rho_i} \right) \frac{\partial \rho_i}{\partial c} \end{Bmatrix} \tag{Va}$$

$$J = \begin{Bmatrix} \frac{\partial^2 \ell}{\partial K_\infty^2} & \frac{\partial^2 \ell}{\partial K_\infty \partial b} & \frac{\partial^2 \ell}{\partial K_\infty \partial c} \\ \frac{\partial^2 \ell}{\partial b \partial K_\infty} & \frac{\partial^2 \ell}{\partial b^2} & \frac{\partial^2 \ell}{\partial b \partial c} \\ \frac{\partial^2 \ell}{\partial c \partial K_\infty} & \frac{\partial^2 \ell}{\partial c \partial b} & \frac{\partial^2 \ell}{\partial c^2} \end{Bmatrix} \tag{Vb}$$

$$\frac{\partial^2 \ell}{\partial \beta_j \partial \beta_k} = \frac{1}{n} \sum_{i=1}^{n} \left(\left(\frac{y_i}{\rho_i} - \frac{1-y_i}{1-\rho_i} \right) \frac{\partial^2 \rho}{\partial \beta_j \partial \beta_k} - \left(\frac{y_i}{\rho_i^2} + \frac{1-y_i}{(1-\rho_i)^2} \right) \frac{\partial \rho}{\partial \beta_j} \frac{\partial \rho}{\partial \beta_k} \right) \tag{Vc}$$

$$\frac{\partial^2 \rho}{\partial K_\infty^2} = 0 \tag{Vd}$$

$$\frac{\partial^2 \rho}{\partial K_\infty \partial b} = -e^{-cx-be^{-cx}} \tag{Ve}$$

$$\frac{\partial^2 \rho}{\partial K_\infty \partial c} = bxe^{-cx-be^{-cx}} \tag{Vf}$$

$$\frac{\partial^2 \rho}{\partial b^2} = K_\infty e^{-2cx-be^{-cx}} \tag{Vg}$$

$$\frac{\partial^2 \rho}{\partial b \partial c} = K_\infty x\left(1-be^{-cx}\right)e^{-cx-be^{-cx}} \tag{Vh}$$

$$\frac{\partial^2 \rho}{\partial c^2} = K_\infty bx^2\left(1-be^{-cx}\right)e^{-cx-be^{-cx}} \tag{Vi}$$

$$u = \frac{1}{n}\begin{Bmatrix} \sum_{i=1}^{n}\left(\frac{y_i}{\rho_i}-\frac{1-y_i}{1-\rho_i}\right)\frac{\partial \rho_i}{\partial K_\infty} \\ \sum_{i=1}^{n}\left(\frac{y_i}{\rho_i}-\frac{1-y_i}{1-\rho_i}\right)\frac{\partial \rho_i}{\partial K_0} \\ \sum_{i=1}^{n}\left(\frac{y_i}{\rho_i}-\frac{1-y_i}{1-\rho_i}\right)\frac{\partial \rho_i}{\partial b} \\ \sum_{i=1}^{n}\left(\frac{y_i}{\rho_i}-\frac{1-y_i}{1-\rho_i}\right)\frac{\partial \rho_i}{\partial c} \end{Bmatrix} \tag{VIa}$$

$$J=\begin{bmatrix} \dfrac{\partial^2 \ell}{\partial K_\infty^2} & \dfrac{\partial^2 \ell}{\partial K_\infty \partial K_0} & \dfrac{\partial^2 \ell}{\partial K_\infty \partial b} & \dfrac{\partial^2 \ell}{\partial K_\infty \partial c} \\ \dfrac{\partial^2 \ell}{\partial K_0 \partial K_\infty} & \dfrac{\partial^2 \ell}{\partial K_0^2} & \dfrac{\partial^2 \ell}{\partial K_0 \partial b} & \dfrac{\partial^2 \ell}{\partial K_0 \partial c} \\ \dfrac{\partial^2 \ell}{\partial b \partial K_\infty} & \dfrac{\partial^2 \ell}{\partial b \partial K_0} & \dfrac{\partial^2 \ell}{\partial b^2} & \dfrac{\partial^2 \ell}{\partial b \partial c} \\ \dfrac{\partial^2 \ell}{\partial c \partial K_\infty} & \dfrac{\partial^2 \ell}{\partial c \partial K_0} & \dfrac{\partial^2 \ell}{\partial c \partial b} & \dfrac{\partial^2 \ell}{\partial c^2} \end{bmatrix} \quad \text{(VIb)}$$

$$\frac{\partial^2 \rho}{\partial K_\infty^2}=\frac{\partial^2 \rho}{\partial K_0^2}=\frac{\partial^2 \rho}{\partial K_\infty \partial K_0}=0 \quad \text{(VIc)}$$

$$\frac{\partial^2 \rho}{\partial K_\infty \partial b}=-\frac{\partial^2 \rho}{\partial K_0 \partial b}=cx\left(bx\right)^{c-1}e^{-\left(bx\right)^c} \quad \text{(VId)}$$

$$\frac{\partial^2 \rho}{\partial K_\infty \partial c}=-\frac{\partial^2 \rho}{\partial K_0 \partial c}=\ln\left(bx\right)\left(bx\right)^c e^{-\left(bx\right)^c} \quad \text{(VIe)}$$

$$\frac{\partial^2 \rho}{\partial b^2}=\left(K_\infty-K_0\right)cx^2 e^{-\left(bx\right)^c}\left(bx\right)^{c-1}\left(2c-\left(c-1\right)\left(bx\right)^{-1}\right) \quad \text{(VIf)}$$

$$\frac{\partial^2 \rho}{\partial b \partial c}=\left(K_\infty-K_0\right)e^{-\left(bx\right)^c}\left(bx\right)^{c-1}x\left(c\ln\left(bx\right)\left(\left(bx\right)^c-1\right)-1\right) \quad \text{(VIg)}$$

$$\frac{\partial^2 \rho}{\partial c^2}=\left(K_\infty-K_0\right)e^{-\left(bx\right)^c}\left(bx\right)^c x\left(c\ln\left(bx\right)-c\ln\left(bx\right)\left(bx\right)^{-1}-\left(bx\right)^{-1}\right) \quad \text{(VIh)}$$

Acknowledgements

The author wishes to acknowledge Dr Marie-Laure Guillemin and Dr Oscar Huanel for providing the *Gracilaria chilensis* data.

Supplementary Material

File Data.mat has the *Gracilaria chilensis* data.

File SCurves1.m fits one curve to a specific data-set using the original ungrouped observations.

File SCurves2.m fits one curve grouping the observations into x classes.

File SCurves3.m fits a curve for each combination of season, site and life cycle stage grouping the observations into x classes.

Acknowledgement

The study was funded by ERDF Funds of the Competitiveness Factors Operational Programme - COMPETE and national funds of the FCT - Foundation for Science and Technology under the project UID/EEA/50009/2013. The funders took no part in the design of the study, in the collection, analysis, and interpretation of data, and in writing the manuscript.

References

Austin SH, Robinson TR, Robinson WD, Ricklefs RE. 2011. Potential biases in estimating the rate parameter of sigmoid growth functions. Methods in Ecology and Evolution, 2(1): 43-51

Barbour AB, Ponciano JM, Lorenzen K. 2013. Apparent survival estimation from continuous mark–recapture/ resighting data. Methods in Ecology and Evolution, 4(9): 846-853

Bates DM, Watts DG. 1988. Nonlinear Regression and Its Applications. Wiley, New York, USA

Borah M, Mahanta SDJ. 2013. Rapid parameter estimation of three parameter nonlinear growth models. International Journal of Mathematical Archive-4(2): 274-282

Dumur D, Pilbeam CJ, Craigon J. 1990. Use of the Weibull function to calculate cardinal temperatures in Faba Bean. Journal of Experimental Botany, 41(11): 1423-1430

Gompertz B. 1825. On the Nature of the Function Expressive of the Law of Human Mortality, and on a New Mode of Determining the Value of Life Contingencies. Philosophical Transactions of the Royal Society of London, 115: 513-585

Guillemin M-L, Sepúlveda RD, Correa JA, Destombe C. 2013. Differential ecological responses to environmental stress in the life history phases of the isomorphic red alga Gracilaria chilensis (Rhodophyta). Journal of Applied Phycology , 25(1): 215-224

Haefner JW. 1996. Modelling Biological Systems: principles and applications. Springer, USA

Jukic D, Kralik G, Scitovski R. 2004. Least-squares fitting Gompertz curve. Journal of Computational and Applied Mathematics, 169(2): 359-375

Kamiya M, Kawai H. 2002. Dependence of the carposporophyte on the maternal gametophyte in three ceramiacean algae (Rhodophyta), with respect to carpospore development, spore production, and germination success. Phycologia, 41: 107-115

King MR, Mody NA. 2010. Numerical and Statistical Methods for Bioengineering: Applications in Matlab. Cambridge University Press, Cambridge, USA

Laird AK. 1964. Dynamics of tumor growth. British Journal of Cancer, 18(3): 490-502

Lange K. 2010. Numerical Analysis for Statisticians (2nd ed). Springer, New York, USA

Levenberg K. 1944. A method for the solution of certain non-linear problems in least squares. Quarterly of

Applied Mathematics, 2: 164-168

Lynch HJ, Fagan WF. 2009. Survivorship curves and their impact on the estimation of maximum population growth rates. Ecology, 90: 1116-1124

Mahanta DJ, Borah M. 2014. Parameter estimation of Weibull growth models in forestry. International Journal of Mathematics trends and Technology, 8(3): 157-163

Marquardt D. 1963. An algorithm for least-squares estimation of nonlinear parameters. SIAM Journal on Applied Mathematics, 11(2): 431-441

Oswald SA, Nisbet ICT, Chiaradia A, Arnold JM. 2012. FlexParamCurve: R package for flexible fitting of nonlinear parametric curves. Methods in Ecology and Evolution, 3(6): 1073-1077

Paine CET, Marthews TR, Vogt DR, Purves D, Rees M, Hector A, Turnbull LA. 2012. How to fit nonlinear plant growth models and calculate growth rates: an update for ecologists. Methods in Ecology and Evolution, 3(2): 245-256

Pletcher SD. 1999. Model fitting and hypothesis testing for age-specific mortality data. Journal of Evolutionary Biology, 12: 430-439

Rosenbaum B, Rall BC. 2018. Fitting functional responses: Direct parameter estimation by simulating differential equations. Methods in Ecology and Evolution, 9(10): 2076-2090

Seber GEF, Lee AJ. 2003. Linear Regression Analysis (Second Edition). John Wiley & Sons, New Jersey, USA

Shafii B, Price WL. 2001. Estimation of cardinal temperatures in germination data analysis. Journal of Agricultural Biological and Environmental Statistics, 6(3): 356-366

Tjørve KMC, Tjørve E. 2017. The use of Gompertz models in growth analyses, and new Gompertz-model approach: An addition to the Unified-Richards family. PLoS ONE, 12(6): e0178691

Vieira VMNCS, Engelen AH, Huanel OR, Guillemin ML. 2016. Linear-in-the-parameters Oblique Least Squares: a case study with the estimation of density-dependent survival in algae with isomorphic biphasic life-cycles. PLoS ONE, 11(12): e0167418

Vieira VMNCS, Engelen AH, Huanel OR, Guillemin ML. 2018. Haploid females in the isomorphic biphasic (haploid-diploid) life-cycle of Gracilaria chilensis excel in survival. BMC Evolutionary Biology, 18: 174

Vieira VMNCS, Engelen AH, Huanel OR, Guillemin ML. 2018. Differentiation of haploid and diploid fertilities in *Gracilaria chilensis* affect ploidy ratio. BMC Evolutionary Biology, 18: 183

Weibull W. 1951. A statistical distribution function of wide applicability. Journal of Applied Mechanics, 18: 293-297

Weisstein EW. Nonlinear Least Squares Fitting. From MathWorld--A Wolfram Web Resource. http://mathworld.wolfram.com/NonlinearLeastSquaresFitting.html. Last updated 31st of July 2018

Wilson KL, Honsey AE, Moe B, Venturelli P. 2018. Growing the biphasic framework: Techniques and recommendations for fitting emerging growth models. Methods in Ecology and Evolution, 9(4): 822-833

Winsor CP. 1932. The Gompertz curve as a growth curve. Proceedings of the National Academy of Sciences of USA, 18: 1-8